The 3-D Multidomain Pseudospectral Time-Domain Method for Wideband Simulation

Gang Zhao, *Student Member, IEEE,* Yan Qing Zeng, and Qing H. Liu, *Senior Member, IEEE*

***Abstract*—A three-dimensional (3-D) multidomain pseudospectral time-domain (PSTD) method with a well-posed PML is developed as an accurate and efficient solver for Maxwell's equations in conductive and inhomogeneous media. The curved object is accurately treated by curvilinear coordinate transformation. Spatial derivatives are obtained by the Chebyshev collocation method to achieve a high-order accuracy. Numerical results show an excellent agreement with solutions obtained by the FDTD method under fine sampling.**

***Index Terms*—FDTD, inhomogeneous objects, PSTD, well-posed PML.**

I. Introduction

THE past decades have seen a rapid growth of the finite-difference time-domain (FDTD) algorithm and its applications to electromagnetic problems. Meanwhile, significant research efforts have been devoted to improving the efficiency and accuracy of the FDTD method. Among such efforts, the pseudospectral methods [1]–[6] have been demonstrated marked advantages in accuracy and efficiency over the FDTD method, and have been applied to inhomogeneous, dispersive, and anisotropic media.

Previously, the Fourier PSTD method, which uses FFT to calculate the spatial derivatives, has been developed by Liu [1], [2]. It demonstrates a remarkable improvement in efficiency and accuracy over the FDTD method, and it requires only two sampling cells per minimum wavelength. However, as pointed out in [1], [2], this algorithm suffers from the Gibbs' phenomenon when applied to perfect conductors, and will incur a staircasing error when applied to curved objects. In order to overcome these limitations, a multidomain Chebyshev pseudospectral time-domain method has been proposed [3], [4]. It employs the Chebyshev polynomials in computing the spatial derivatives. The Chebyshev PSTD algorithm has shown the capacity of solving problems in complex geometries with a great flexibility, though it slightly increases computational burden because about π points per minimum wavelength are needed to accurately resolve a wave.

In this paper, we focus on developing the 3-D multidomain Chebyshev PSTD method for inhomogeneous and lossy media as well as for perfect conductors. A 3-D well-posed PML is introduced for the truncation of the computational domain, and the physical conditions are used as subdomain patching conditions on the interface of subdomains. This work is an extention of the earlier research on the PSTD algorithm [3]–[6].

Manuscript received August 6, 2002; revised October 22, 2002. This work was supported by the National Science Foundation under Grants CCR-00-98140 and IIS-0086075. The review of this letter was arranged by Associate Editor Dr. Shigeo Kawasaki.

The authors are with the Department of Electrical and Computer Engineering, Duke University, Durham, NC 27708-0291 USA (e-mail: qhliu@ee.duke.edu.).

Digital Object Identifier 10.1109/LMWC.2003.811667

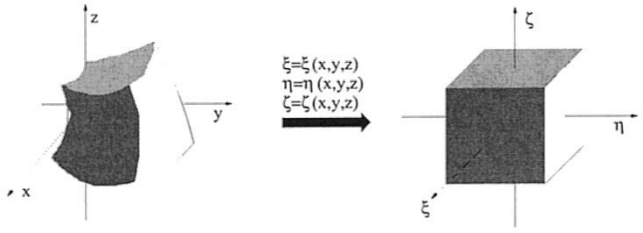

Fig. 1. Coordinates transformation for each curved hexahedral subdomain.

II. Theory

Consider an isotropic, conductive, inhomogeneous medium with permittivity ϵ, permeability μ, and conductivity σ. Maxwell's equations for such a lossy medium are

$$\nabla \times \mathbf{E} = -\mu \frac{\partial \mathbf{H}}{\partial t} \tag{1}$$

$$\nabla \times \mathbf{H} = \epsilon \frac{\partial \mathbf{E}}{\partial t} + \sigma \mathbf{E} + \mathbf{J}. \tag{2}$$

In order to treat curved objects, the computational domain is first decomposed into a series of hexahedral subdomains naturally conformal with the problem geometry. Then, a curvilinear coordinate transformation is performed to map a curved hexahedral subdomain in (x, y, z) coordinates into a unit cube in (ξ, η, ζ) coordinates, as shown in Fig. 1.

With the transform relation

$$\xi = \xi(x,y,z), \qquad \eta = \eta(x,y,z), \qquad \zeta = \zeta(x,y,z) \tag{3}$$

Maxwell's equations (1) and (2) in a source free region can be written in the matrix form as follows:

$$\sqrt{\epsilon\mu}\frac{\partial q}{\partial t} + A\frac{\partial q}{\partial \xi} + B\frac{\partial q}{\partial \eta} + C\frac{\partial q}{\partial \zeta} + Dq = 0 \tag{4}$$

where $q = [H_x/\sqrt{\epsilon}, H_y/\sqrt{\epsilon}, H_z/\sqrt{\epsilon}, E_x/\sqrt{\mu}, E_y/\sqrt{\mu}, E_z/\sqrt{\mu}]^T$,

$$A = \begin{pmatrix} 0 & 0 & 0 & 0 & -\xi_z & \xi_y \\ 0 & 0 & 0 & \xi_z & 0 & -\xi_x \\ 0 & 0 & 0 & -\xi_y & \xi_x & 0 \\ 0 & \xi_z & -\xi_y & 0 & 0 & 0 \\ -\xi_z & 0 & \xi_x & 0 & 0 & 0 \\ \xi_y & -\xi_x & 0 & 0 & 0 & 0 \end{pmatrix} \tag{5}$$

$$D = \text{diag}\left(0,\ 0,\ 0,\ \sigma\sqrt{\frac{\mu}{\epsilon}},\ \sigma\sqrt{\frac{\mu}{\epsilon}},\ \sigma\sqrt{\frac{\mu}{\epsilon}}\right) \tag{6}$$

and B and C have a similar form as A.

After transformation onto the (ξ, η, ζ) coordinates, the sampling points within each unit cube are located at the Chebyshev-Gauss-Lobatto collocation points

$$\begin{aligned}\xi_i &= -\cos\left(\frac{i\pi}{I}\right), \quad i = 0, 1, \ldots I \\ \eta_j &= -\cos\left(\frac{j\pi}{J}\right), \quad j = 0, 1, \ldots J \\ \zeta_l &= -\cos\left(\frac{l\pi}{L}\right), \quad l = 0, 1, \ldots L. \end{aligned} \tag{7}$$

A field component $f(\xi, \eta, \zeta)$ defined in the unit cube is interpolated by the Chebyshev-Lagrange interpolation polynomials $g_i(\xi)$, $g_j(\eta)$, and $g_l(\zeta)$ as

$$f(\xi, \eta, \zeta) = \sum_{i=0}^{I}\sum_{j=0}^{J}\sum_{l=0}^{L} f(\xi_i, \eta_j, \zeta_l)\, g_i(\xi) g_j(\eta) g_l(\zeta) \tag{8}$$

where, for example, the interpolation polynomial $g_i(\xi)$ is

$$g_i(\xi) = \frac{\left(1-\xi^2\right) T_I'(\xi)(-1)^{i+1}}{c_i I^2 (\xi - \xi_i)} \tag{9}$$

and $c_0 = c_I = 2$ and $c_i = 1$ for $1 \le i \le I-1$, and the Ith order Chebyshev polynomial is defined as $T_I(\xi) = \cos(I \cos^{-1}\xi)$. The partial derivatives of $f(\xi, \eta, \zeta)$ with respect to ξ, η and ζ are approximated as

$$\frac{\partial f(\xi_i, \eta_j, \zeta_l)}{\partial \xi} = \sum_{k=0}^{I} D_{ik}^{(\xi)} f(\xi_k, \eta_j, \zeta_l), \tag{10}$$

$$\frac{\partial f(\xi_i, \eta_j, \zeta_l)}{\partial \eta} = \sum_{k=0}^{J} D_{jk}^{(\eta)} f(\xi_i, \eta_k, \zeta_l), \tag{11}$$

$$\frac{\partial f(\xi_i, \eta_j, \zeta_l)}{\partial \zeta} = \sum_{k=0}^{L} D_{lk}^{(\zeta)} f(\xi_i, \eta_j, \zeta_k) \tag{12}$$

where the differential matrix element is defined as [4], [5]

$$D_{ik}^{(\alpha)} = g_k'(\alpha_i), \qquad \alpha = \xi, \eta, \zeta, \qquad i, k = 0, 1, \ldots I_\alpha. \tag{13}$$

To absorb the outgoing waves for the finite computational domain, we use a 3-D well-posed PML for lossy media derived by Fan and Liu [7]. Incidentally, this work can be viewed as the first implementation and validation for their 3-D PML formulations.

For the multidomain scheme, a special step called subdomain patching is always necessary to exchange information between the individual subdomains to match the boundary conditions at their interfaces. This procedure is performed at each stage of time integration after the field components are updated. In this work, we use the physical conditions to achieve this aim. First, the tangential components of electric and magnetic fields are extracted as follows:

$$\begin{aligned} H_{t1} &= \mathbf{H}\cdot\mathbf{t_1}, \quad H_{t2} = \mathbf{H}\cdot\mathbf{t_2}, \quad H_n = \mathbf{H}\cdot\mathbf{n} \\ E_{t1} &= \mathbf{E}\cdot\mathbf{t_1}, \quad E_{t2} = \mathbf{E}\cdot\mathbf{t_2}, \quad E_n = \mathbf{E}\cdot\mathbf{n} \end{aligned} \tag{14}$$

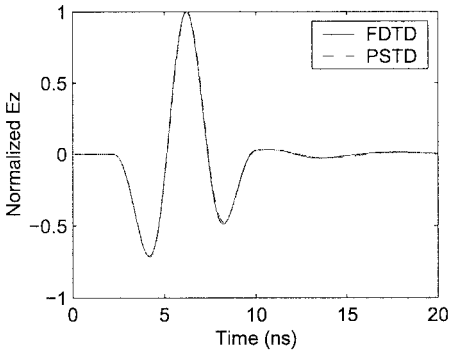

Fig. 2. Radiation of an electric dipole source outside a PEC cube.

where $\mathbf{t_1}$, $\mathbf{t_2}$ and $\mathbf{n}$ are local unit tangential and normal vectors. Then, the tangential components are forced to be continuous between two adjacent subdomains

$$\begin{aligned} {H_{t1}}^{(1)}, {H_{t1}}^{(2)} &\Longleftarrow \frac{\left({H_{t1}}^{(1)} + {H_{t1}}^{(2)}\right)}{2} \\ {H_{t2}}^{(1)}, {H_{t2}}^{(2)} &\Longleftarrow \frac{\left({H_{t2}}^{(1)} + {H_{t2}}^{(2)}\right)}{2} \\ {E_{t1}}^{(1)}, {E_{t1}}^{(2)} &\Longleftarrow \frac{\left({E_{t1}}^{(1)} + {E_{t1}}^{(2)}\right)}{2} \\ {E_{t2}}^{(1)}, {E_{t2}}^{(2)} &\Longleftarrow \frac{\left({E_{t2}}^{(1)} + {E_{t2}}^{(2)}\right)}{2} \end{aligned} \tag{15}$$

where the superscripts signify the two adjacent subdomains, and the normal components are left unchanged. On the other hand, for a surface adjacent to the perfect conductor, the tangential components of electric fields and the normal component of magnetic fields are forced to be zero, and the tangential components of magnetic fields remain continuous.

III. Numerical Results

In following 3-D PSTD results (except the first example), we use a grid of $8 \times 8 \times 8$ points for each hexahedron, and a 2-stage 2nd order Runge-Kutta method for time integration. The Blackman-Harris window function is chosen as the time function of the plane wave source and the dipole source for all examples.

Resonant Frequency of a PEC Cavity: A cubic PEC cavity with a side length of 1.8 m is excited by an electrical dipole source located at the center of the cavity; the central frequency of the time function is 200 MHz. After the time-domain waveform for the wide-band signal is obtained by PSTD, we use Fourier transform to obtain its spectrum. From the spectrum, an obvious peak at 118.0 MHz is observed, which corresponds to the resonant frequency and well agrees with the theoretical value 117.9 MHz (error $< 0.09\%$). The sampling density of the PSTD method is 5.65 points per wavelength (PPW) with $4 \times 4 \times 4$ cells.

A PEC Cube: We now consider the fields due to an electric dipole source, $\mathbf{J} = \hat{z}\delta(z - 0.6)\delta(x)\delta(y)$ outside a PEC cube with side length of 0.6 m. The central frequency of the source is 200 MHz. The cube is centered at (0, 0, −0.6) m, and the

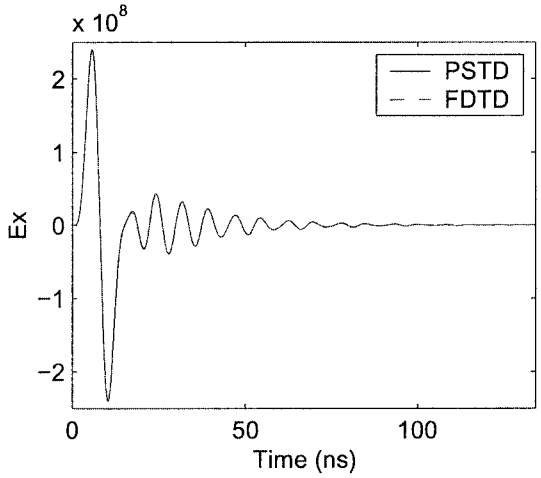

Fig. 3. Scattering of a plane wave from a dielectric cube of $\epsilon_r = 9$.

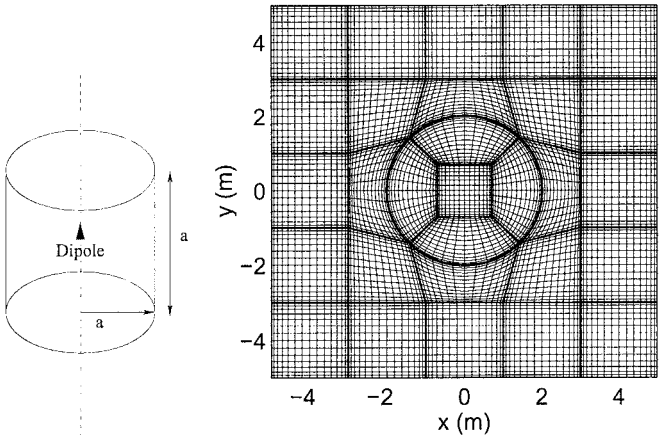

Fig. 4. Dielectric circular cylinder ($a = 2.0$ m) and its meshed transverse section.

observation point is located at (0.6, 0, 0.3) m. The simulation results of PSTD (8 PPW) and FDTD (20 PPW) are compared in Fig. 2 and very good agreement is observed.

A Dielectric Cube: The third example considers the fields due to a plane wave with a central frequency of 100 MHz incident along $+z$ direction with the electric field polarized in x direction. The incident wave is scattered by a dielectric cube with $\epsilon_r = 9$ and the side length $a = 0.6$ m. The observation point is located at (0, 0, -0.6) m. Fig. 3 presents the numerical results of PSTD (5.3 PPW) and FDTD (13.3 PPW), showing an excellent agreement.

A Circular Cylinder: The PSTD method is ideal for modeling curved objects such as the circular cylinder structure shown in Fig. 4. In this case, it has a size $a = 2$ m with $\epsilon_r = 2.56$; the mesh in the transverse section is shown to illustrate the conformal grid. An electric dipole source $\mathbf{J} = \hat{z}\delta(z)\delta(x)\delta(y)$ is located at the center of cylinder with a

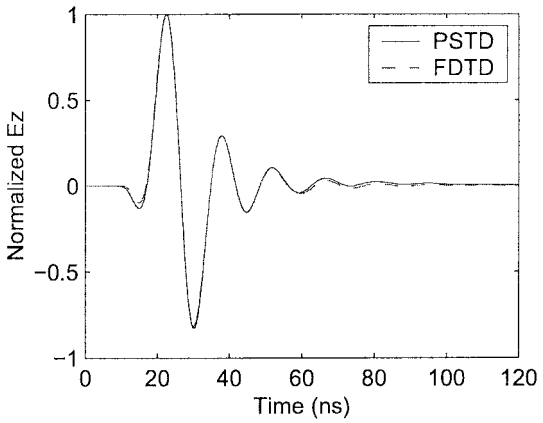

Fig. 5. Radiation of an electric dipole source in the dielectric circular cylinder in Fig. 4.

central frequency of 60 MHz. The location of observation point is (1, -1, 2) m. As can be seen in Fig. 5, the simulation results of PSTD (3.18 PPW) agree very well with the results of FDTD (12.5 PPW).

IV. Conclusions

A 3-D multidomain pseudospectral time-domain algorithm has been developed for inhomogeneous objects and perfect conductors. A 3-D well-posed PML has been implemented and validated in this work, and the physical boundary conditions have been developed as the subdomain patching strategy for the multidomain algorithm. Numerical results show a very good agreement between the 3-D multidomain PSTD and FDTD results, even when the sampling density of the PSTD is close to π points per wavelength.

References

[1] Q. H. Liu, "A spectral-domain method with perfectly matched layers for time-domain solutions of Maxwell's equations," in 1996 URSI Meeting, Baltimore, MD, July 1996.

[2] ——, "The PSTD algorithm: A time-domain method requiring only two cells per wavelength," *Microwave Opt. Technol. Lett.*, vol. 15, pp. 158–165, 1997.

[3] B. Yang, D. Gottlieb, and J. S. Hesthaven, "Spectral simulation of electromagnetic wave scattering," *J. Comput. Phy.*, vol. 134, pp. 216–230, 1997.

[4] B. Yang and J. S. Hesthaven, "A Pseudospectral method for time-domain computation of electromagnetic scattering by bodies of revolution," *IEEE Trans. Antennas and Propagat.*, vol. 47, pp. 132–141, 1999.

[5] G.-X. Fan, Q. H. Liu, and J. S. Hesthaven, "Multidomain pseudospectral time-domain method for simulation of scattering from objects buried in lossy media," *IEEE Trans. Geosci. Remote Sensing*, vol. 40, pp. 1366–1373, June 2002.

[6] G. Zhao and Q. H. Liu, "The 2.5-D multidomain pseudospectral time-domain algorithm," *IEEE Trans. Antennas Propagat.*, vol. 50, 2003, to be published.

[7] G.-X. Fan and Q. H. Liu, "A well-posed PML absorbing boundary condition for lossy media," in *IEEE Antennas and Propagat. Soc. Int. Symp.*, vol. 3, July 2001, pp. 2–5.